Antigen-specific Memory T Cell Distribution in Non-Lymphoid Tissue

by

Mobolaji O. Olurinde

B.S. Chemical Engineering (Highest Honors)
B.S. Agricultural & Biological Engineering (Honors)
University of Florida, 2002

SUBMITTED TO THE DEPARTMENT OF BIOLOGICAL ENGINEERING IN PARTIAL FULFILLMENT OF THE REQUIREMENTS FOR THE DEGREE OF

MASTER OF SCIENCE IN BIOLOGICAL ENGINEERING
AT THE
MASSACHUSETTS INSTITUTE OF TECHNOLOGY

SEPTEMBER 2007

Signature of Author.....
Department of Biological Engineering
June 25, 2007

Certified by.....
Paul T. Matsudaira
Professor of Biology & Biological Engineering
Thesis Supervisor

Certified by.....
Jianzhu Chen
Professor of Biology
Thesis Supervisor

Accepted by.....
Alan J. Grodzinsky
Professor of Electrical, Mechanical & Biological Engineering
Chair, Course 20 Graduate Program Committee

Antigen-specific Memory T Cell Distribution in Non-Lymphoid Tissue

by

Mobolaji O. Olurinde

Submitted to the Department of Biological Engineering
on June 25, 2007 in Partial Fulfillment of the
Requirements for the Degree of Master of Science in
Biological Engineering

ABSTRACT

CD8+ T cells are the main adaptive immune system cell type responding to intracellular pathogens, particularly viruses, and tumor antigens. In the case of influenza, activated T cells migrate from the mediastinal (draining) lymph nodes to the lung where they perform their cytolytic function. After pathogen clearance, memory CD8+ T cells are generated, giving rise to long-term protection from reinfection. However, these cells are no longer detectable in the lung parenchyma six months post-infection, and cell-mediated immunity, and protection is lost. Knock-out studies in mice show that interleukin 15 (IL-15) is essential for memory CD8+ T cell proliferation. Fibroblasts, macrophages, dendritic cells and epithelial cells express IL-15 and its receptor isoform α (IL-15Rα). Histological studies suggest that memory CD8+ T cells preferentially reside in peribronchiolar and perivascular areas, the stroma, of the lung. We hypothesize that memory CD8+ T cells preferentially reside in regions where molecules necessary for their maintenance, for example, IL-15/R secreting cells, are located. In this study, we have shown that antigen-specific 2C GFP effector memory CD8+ T cells are generated in B6 recipient mice 30-32 days after influenza virus infection, preferentially reside in peribronchiolar areas. Both 2C and 2C GFP recipient mice have severe vasculitis and widely distributed inflammatory infiltrates 7 days post-infection. Lower lung lobes appear to be more affected than upper lobes at this time point. On day 30, most of the airways have been cleared and restored. Although lymphoid-appearing nodules were detected in the lungs 31 dpi, no clusters of B cells and T cells suggesting induced BALT were identified by immunofluorescence. Interestingly, antigen-specific GFP cells preferentially remained in the lung tissue and were almost undetectable in spleens, lymph nodes, and livers. This preference was not observed in 2C (non-GFP) recipient mice. Immunofluorescence studies showed no colocalization between 2C GFP T cells and dendritic cells that might suggest stable dendritic cell interactions contribute to antigen-specific cells preferentially residing in the lung stroma. Further studies are necessary to determine what other cell types might contribute to this phenomenon. These results provide some insight into how structural elements in non-lymphoid tissue influence cell-mediated immunity.

Thesis Supervisor: Paul T. Matsudaira
Title: Professor of Biology & Biological Engineering

Thesis Supervisor: Jianzhu Chen
Title: Professor of Biology

BIOGRAPHICAL NOTE

Mobolaji O. Olurinde, a native of Nigeria, graduated from University of Florida (UF) in December 2002 with Bachelor of Science degrees in Chemical Engineering (Highest Honors) and Biological Engineering (Honors). During her academic career at UF, she received multiple awards and scholarships for academic excellence, and exemplary leadership and community service. Some of these awards include Gator Engineering 4-year Scholar, College of Engineering Leadership Award, Who's Who in American Universities and Colleges, and the United States Achievement Academy All-American Scholar. She served as Academic Excellence Co-chair and Vice President of Communications for the National Society of Black Engineers (NSBE) UF Chapter, Historian of the North Star Leadership Council, and Secretary and President of the National Organization for the Professional Advancement of Black Chemists and Chemical Engineers (NOBCChE) UF Chapter. She demonstrated her commitment to promote scholastic excellence, particularly amongst minority students, by mentoring and tutoring pre-collegiate and collegiate students in mathematics and sciences through the Upward Bound program, the College of Engineering STEPUP program, and the Gateway Christian Tutoring Program. Before moving to Boston after graduation, she tutored predominantly black students in the JPMC After-School Youth Program, Miami, Florida. She also volunteered at the Shands Hospital emergency room and pediatric immunology clinic in Gainesville while at UF. She is a member of the Golden Key National Honor Society, the National Society of Collegiate Scholars, the Massachusetts Medical Society, and the American Association for the Advancement of Science (AAAS). While in Boston, she has volunteered in the Harvard Mentoring for Science Grade 8 program, the Tremont Temple Baptist Church (TTBC) Christian Education Ministry, and the TTBC Chancel Choir. She enjoys singing, dancing, photography, and arts/crafts-making.

Mobolaji discovered her joy for doing research during her 2000 summer internship at Dow Chemical Company, Freeport, Texas where she designed and carried out experiments to determine the effects of corona treatment on some Dow brand Polyethylene films. After this internship experience, she promptly sought out other research opportunities. The first, a research project at University of California, San Francisco, involved predicting the mechanism for toxicity in users of arylpropionic acid Nonsteroidal Anti-inflammatory Drugs. Results of this project are published in Drug Metabolism and Disposition Journal June 2003 issue. Her second project at the University of Florida studied interaction forces between nano-sized particles and a flat surface using a single-beam gradient optical trap and evanescent wave light scattering technique. In the summer of 2002, she worked at Dow AgroSciences, identifying and purifying a novel protein that will be used to create crops resistant to insect pests. Mobolaji received the National Science Foundation (NSF) Graduate Research Fellowship in 2003. She enrolled in the Harvard Medical School Pre-Matriculation Summer Program in 2003, where she assisted in isolating human single chain variable fragment (scFv) antibodies against Severe Acute Respiratory Syndrome (SARS) S1 protein. Results of this project are published in PNAS February 2004 issue. She is currently enrolled in the Harvard-MIT Health Sciences and Technology Medical Degree (MD) and Medical Engineering Medical Physics (MEMP) programs.

TABLE OF CONTENTS

I.INTRODUCTION

CD8+ T cells are the main adaptive immune system cell type responding to intracellular pathogens, particularly viruses, and tumor antigens [1-6]. In the case of influenza virus infection, antigen is carried by antigen-presenting cells (APCs) to the mediastinal lymph nodes (MedLN) where these cells present antigen to naïve CD8+ T cells [2, 4, 7-14]. Activated antigen-specific T cells remain in the lymph nodes and proliferate during the first three-four days post-infection [2, 7-15]. Activated T cells then exit the lymph node through the efferent lymph vessel into peripheral tissues, including the inflamed tissue of the lung [4, 7, 10, 16-22].

Mononuclear infiltrates (lymphocytes, granulocytes and macrophages) are observed in histological sections of the alveoli, bronchi, and upper airways of the lung, completely defacing the lung morphology between days 5-8 [23-25]. When virus is cleared, usually in less than two weeks post-infection, the lung pathology is often restored to 'normal' with mononuclear infiltrates observed only in the lung airways, and peribronchiolar and perivascular areas of the lung parenchyma [23, 26, 27].

By day 30 post-infection, the T cells in the lung have acquired memory phenotypic markers and persist in this tissue [28, 29]. Memory CD8+ T cells are necessary for long-term immunity to viral infections [30-33]. Recall responses to subsequent infections by the same or similar viral antigen is often rapid, leading to faster recovery from illness [1, 34-36]. In the case of influenza, however, the memory cells in the lung parenchyma decline in numbers over a period of six months or less [27, 36, 37] and cell-mediated immunity to influenza virus is lost. The reason for this decline is unknown.

Several studies have shown that cytokines, especially interleukin (IL)-7 and IL-15, are necessary for survival and proliferation of memory T cells [38-42]. IL-15 deficient (IL-15-/-) and

IL-15 receptor isoform α deficient (IL-15Rα-/-) mice have substantially lower numbers of naïve and memory CD8+ T cells compared to wild-type mice [43-48]. In inflammatory diseases that affect the intestine or the lung, high levels of IL-15 have been correlated with persistent lymphocyte populations [49, 50]. This suggests IL-15 is essential for maintaining memory CD8+ T cell numbers.

Memory CD8+ T cells persist in non-lymphoid tissue despite the absence of secondary lymphoid organs [51, 52]. These results suggest an important role for at least a subset of non-lymphoid organs such as the lung in the survival of memory T cells. Most of these studies were performed using tissues that have been processed for flow cytometry or biochemical studies, and do not provide any information about the spatial distribution of memory cells in tissue. The structural network in the lung might explain why memory CD8+ T cells are located in peribronchiolar and perivascular areas of that organ [23, 27, 53]. Identifying the structural elements that control the location of memory T cells may shed more light on the differences that have been observed between T cell maintenance in lymphoid versus non-lymphoid tissue [54, 55]. It may also address the lack of persistence of lung resident memory cells following an immune challenge.

No one has related the spatial distribution of memory CD8+ T cells to their maintenance in non-lymphoid tissues. Hogan et al. [27] showed that CD8+ CD44+ T cells are found in the peribronchiolar epithelial regions of the lung 60 days after influenza A/PR8 infection. Hematoxylin-and-eosin (H&E) stained sections viewed at earlier time points, within days after viral replication stops, also suggest that T cells preferentially reside around the bronchial epithelium [23, 27, 53]. The stroma is responsible for support; providing cytokines, adhesion molecules, and nutrients to ensure cell survival. The lung stroma is comprised of collagen types

I, III, and VI [56-58]. Fibroblasts are the main cell types that synthesize collagen; a major protein component of the extracellular matrix. Epithelial cells can also synthesize collagen. Kim JK et al. [59] showed that collagen type III has α1β1 (VLA-1) and α2β2 sites that are needed for adhesion to human lung fibroblast cells. Also, Ray SJ et al. [60] showed that VLA-1 is needed for recruitment and retention of memory T cells into the lung in an influenza mouse model. Since collagen type III is most abundant in the peribronchiolar and perivascular regions [56], it is likely that fibroblasts would interact closely with memory CD8+ T cells in the lung.

At peripheral tissue sites, fibroblast-like cells [61-63], dendritic cells [64], and macrophages [50, 65], are sources of IL-15 and IL-15Rα. The human respiratory epithelial cell line A549 expresses IL-15Rα [66]. Recently, it was shown that there is a cell-surface bound isoform of IL-15Rα, and both IL-15 and IL-15Rα are produced by the same cells [67], suggesting that IL-15 is secreted in a transpresentation model [68]. That is, IL-15 secreting cells have both the ligand and the α subunit of the receptor [68, 69]. The target cells must have the IL-2Rβ and common-γ chain receptor subunits in order to respond to IL-15 signals [69].

Since IL-15 and IL-15Rα are produced by the same cells, and memory CD8+ T cells require IL-15 to proliferate, I hypothesize that memory CD8+ T cells in the lung are maintained in peribronchiolar and perivascular regions where cells expressing molecules such as IL-15 and IL-15Rα that are necessary for their maintenance can be found. Recent studies suggest majority of the IL-15Rα positive cells in homogenized lung tissue appear to be nonhematopoietic cells [70]. However which of these cells is important in memory cell maintenance remains to be elucidated.

Several groups have shown that CD8+ T cell interactions in tissue can be investigated using microscopy [9, 12, 71]. This approach allows one to visually determine the location of a cell with respect to its neighbors. In our influenza mouse model, WSN-SIY, a mouse-specific

recombinant H1N1 influenza virus strain with the SIYRYYGL (SIY) epitope engineered into the neuraminidase (NA) stalk is recognized by 2C TCR expressing cells when the epitope is presented on K^{b+} APCs or virus-infected target cells [72]. This system allows controlled numbers of 2C T cells responding to a defined epitope (SIY) to be introduced into a mouse by adoptive transfer. 2C T cells are isolated from transgenic mice on a recombination activating gene-1 deficient (RAG1-/-) background (2C RAG-/-). These cells can be further engineered by introducing other knockouts or transgenes onto the 2C RAG-/- background. In this project we are able to study cell trafficking by introducing GFP [73] to allow individual cells to be easily tracked by microscopy. This allows us greater versatility and flexibility in cell tracking to study the location and potential interaction partners of memory CD8+ T cells in the lung than others have previously done. Compared to organic fluorophores often used to perform antigen-specific T cell interaction studies, our GFP system could be used to track antigen-specific cells long-term (>7 days post-transfer).

In this thesis, we validate the ability of this model to study memory T cell response to influenza infection, and determine where antigen-specific cells are located in lung tissue. In addition, because of the ease of staining for dendritic cells and knowing that dendritic cells also secrete IL-15 [64], we investigated whether T cells are closely associated with resident dendritic cells in the lung. These studies provide a basis for exploring the role of different cell types in memory CD8+ T cell maintenance in the lung.

II. VALIDATING THE EXPERIMENTAL MODEL

A. Methods

Mice and Viruses: 2C TCR GFP-expressing and 2C TCR (without GFP) transgenic mice on RAG1-/- and B6 background were maintained at the Massachusetts Institute of Technology (MIT) Animal Care Facility. Recipient B6 mice, ages 8-14 weeks old, were either maintained in the MIT facility or purchased from Taconic Farms, Inc. (Hudson, NY). Recombinant WSN (H1N1) influenza virus with SIYRYYGL peptide engineered onto the neuraminidase stalk originally constructed by plasmid-based reverse genetics [74] was grown on Madine-Darby Canine Kidney (MDCK) cells.

Antibodies & Reagents: Biotinylated 1B2 monoclonal antibody was produced in-house. 1B2 is a monoclonal antibody specific for the 2C TCR. Other anti-mouse monoclonal antibodies (anti-mouse CD16/32, CD8a-APC, CD8a-PE, Streptavidin-APC, Streptavidin-FITC, CD44-PE, CD62L-APC) for flow cytometry studies were purchased from either BioLegend (San Diego, CA) or BD Biosciences (San Jose, CA). Propidium iodide P4170 (PI) was acquired from Sigma-Aldrich (USA).

Lymphocyte Isolation (Lymph Nodes and Spleen): Lymph nodes (LNs) from 2C RAG-/- and 2C GFP RAG-/- mice were extracted, one mouse at a time, after carbon dioxide (CO_2) asphyxiation. The sacrificed animal's fur was sterilized with 70% ethanol. The LNs were extracted by dissection and stored on ice in 4 ml of RPMI 1640 media supplemented with 5% fetal bovine serum and 10 mM HEPES buffer solution (RPMI complete). After dissection, the LNs were gently mashed between rough surfaces of two microscope slides immersed in RPMI

complete to release lymphocytes. Slides were rinsed with additional 1-2 ml of RPMI complete, filtered through sterile gauze and transferred into 15-ml Falcon tubes. A similar procedure was followed for cell isolation from the spleen. Splenocytes were further purified by a red blood cell (RBC) lysis step after mashing.

Lymphocyte Extraction (Lung and Liver): To extract cells from the lungs and liver, each specimen was ground through a cell strainer in 15 ml of RPMI complete. Then the suspension was centrifuged and resuspended in 2 mg/ml Collagenase A (from Roche) in RPMI complete solution. Lungs were digested in 2 ml of Collagenase A solution while liver specimens each contained 3 ml of the solution. The tissue was digested for 1 hr in a 37 ^{o}C water bath. An equal volume of 70% Percoll was added to the digest followed by centrifugation at ~2000 rpm for 20 min. The tissue debris and supernatant was gently aspirated, and RBC lysis was undertaken.

Red blood cell (RBC) Lysis: Two milliliters of red blood cell lysis buffer (144 mM ammonium chloride and 17 mM Tris-HCl pH7.4 in distilled deionized water) was added to the pellet and kept on ice for 3-5 min. Ten millimeters of RPMI complete was added to stop the lysis. Cell suspensions were centrifuged at ~1220 rpm and resuspended in an appropriate buffer for further analysis, filtered through a nylon mesh (Sefar) into appropriately labeled tubes and kept on ice.

Cell counting: The total number of viable cells for each tissue specimen was counted using a hemacytometer and tryphan blue exclusion.

***Flow Cytometry*:** Appropriate numbers of counted cells in suspension were transferred into labeled Falcon® round-bottom tubes (FACS tubes), and centrifuged at ~1210 rpm for 5 min. All procedures were performed on ice. Antibodies of 1:100 dilutions in FACS buffer (1% BSA and 0.1% sodium azide in 1x PBS) were used for staining. Purified anti-mouse CD16/32 (BioLegend), the Fc blocker, was added for 10 min prior to adding the primary antibody. Cells were incubated with the primary antibody on ice for 30 min, washed and then incubated with the secondary and fluorophore-conjugated antibodies for 15 min while covered with foil paper. The cells were washed again, and resuspended in 0.2 μg/ml propidium iodide solution (1:500 dilution). Samples were sorted using a BD FACSCalibur™ flow cytometer (BD Biosciences). Further data analysis was carried out using FlowJo software (Tree Star, Inc., Ashland, OR).

Cell Transfer & Influenza Infection: Cells were resuspended in Hank's Balanced Salt Solution (serum-free media), filtered and kept on ice. Following approved animal care facility protocol, recipient B6 mice were anesthetized with 2.5% Avertin, and injected retroorbitally with 2 x 10^6 total live cells suspended in 100 μl isolated from 2C or 2C GFP lymph nodes as described above. This number corresponds to an average of about 4 x 10^5 naïve 2C CD8+ T cells per mouse. Under anesthesia, mice were intranasally infected, either immediately or in less than 24 hrs after the cell transfer, with 100 pfu of WSN-SIY influenza virus suspended in 50 μl.

B.Results

Figure 1 shows an example plot of naïve 2C and 2C GFP lymphocytes analyzed by flow cytometry before the cells were transferred into B6 recipient mice. Generally, naïve 2C GFP cells are more than 60% of the isolated CD8+ population.

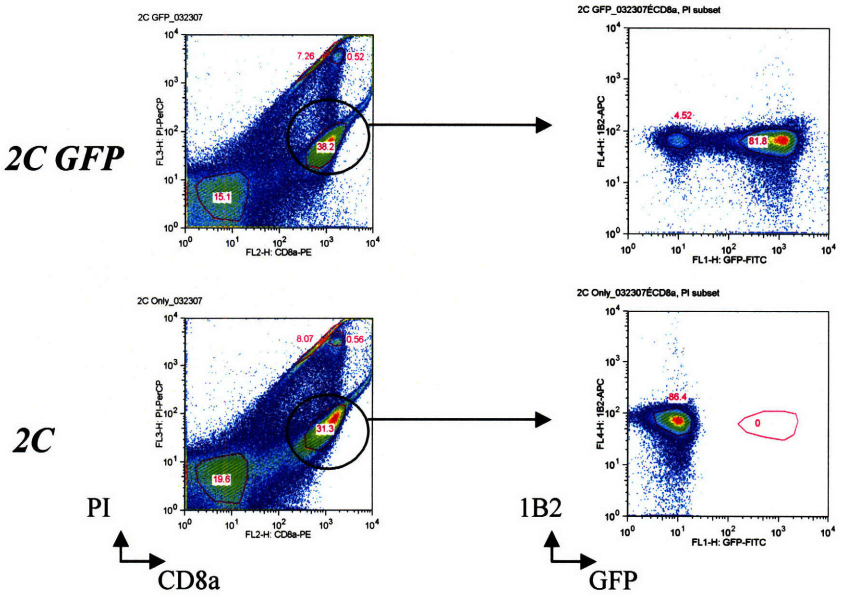

Fig. 1. Naïve 2C GFP CD8+ cells are a distinct population identified by flow cytometry analysis. Plot shows isolated cells from lymph nodes of 2C GFP RAG1-/- (top row) and 2C RAG1-/- (bottom row) mice. Both cell populations were stained with biotinylated 1B2, Streptavidin-APC, and CD8a-PE antibodies. Propidium iodide (PI) staining was used to identify dead cells. Cells were sorted using a BD FACSCalibur™ flow cytometer and the data was analyzed with FlowJo software. Cells were gated on PI versus CD8a+ staining (left panel). Then, PI^{low} and $CD8a^{high}$ populations were selected and analyzed for 1B2 staining and GFP expression (right panel).

Seven days post-infection, GFP lymphocytes are 1B2+ and CD8+, and are present in both lymphoid and non-lymphoid tissues (Fig. 2 and Table I). Greater than 90% of the GFP-expressing cells in the lung are 1B2+ and CD8+ (Fig. 2a).

(a)

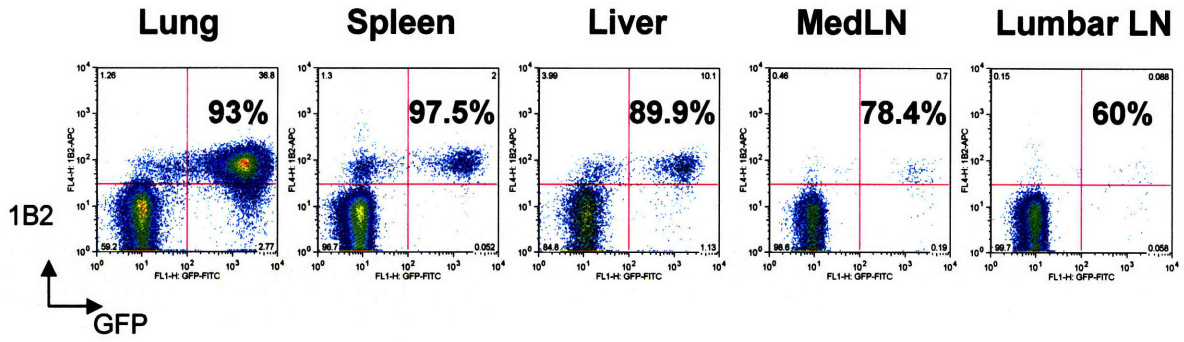

(b)

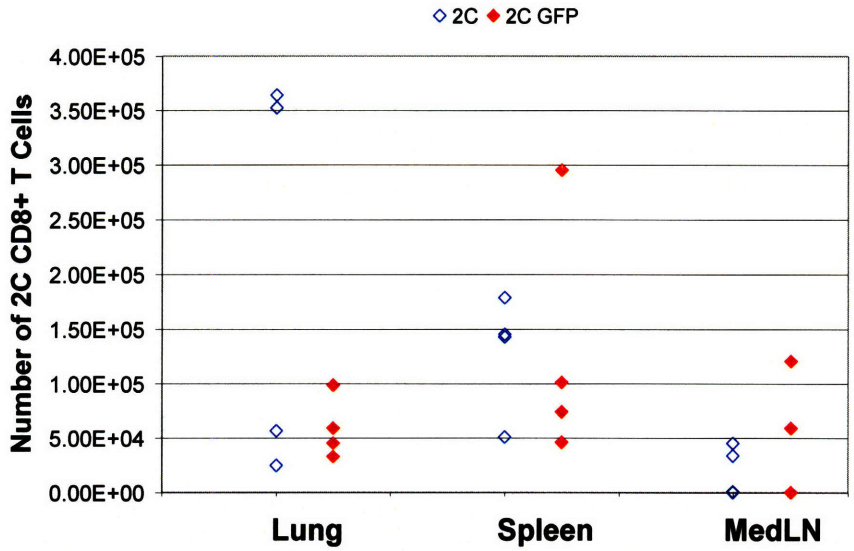

Fig. 2. Distribution of antigen-specific 2C GFP Cells 7 days after 100 pfu of WSN-SIY Influenza infection. **(a)**Representative plot showing the distribution of CD8a+ 1B2+ GFP cells in different tissues for one mouse. The percentages are the ratios of CD8a+ 1B2+ GFP cells to total CD8a+ GFP cells. **(b)** Chart shows the total number of 1B2+ CD8a+ lymphocytes isolated per mouse. Each dot in (b) represents one mouse. There are 4 mice per group in two independent experiments. Cells were isolated and stained with Biotinylated 1B2, Streptavidin-APC, and CD8a-PE antibodies, as well as with PI for flow cytometry as described in the methods section. Analysis was performed using FlowJo software. Cells were gated on PI versus CD8a expression. Then, PI^{low} and $CD8a^{high}$ populations were gated on Side versus Forward scatter plots to eliminate residual erythrocytes and granulocytes. The lymphocyte population selected was analyzed further for 1B2 and GFP expression. LN stands for lymph nodes. MedLN represents mediastinal draining lymph nodes. Lumbar LN is an example of a non-draining lymph node.

Table I. Average numbers of antigen-specific cells in 2C and 2C GFP recipient B6 mice 7 days after influenza infection. Cells were isolated and stained with Biotinylated 1B2, Streptavidin-APC, and CD8a-PE antibodies, as well as with PI for flow cytometry as described in the methods section. Analysis was performed using FlowJo software and Microsoft Excel. The standard deviation is given for groups that have 4 mice per group. Others have only 2 mice per group. LN represents lymph nodes. MedLN is an abbreviation for mediastinal draining lymph nodes.

Tissue	Donor Cell Type	Total Number of Cells	Number of CD8+ Cells	Number of CD8+ 1B2+ Cells	Ratio of CD8+1B2+ Cells to total CD8+ cells (%)
Lung	2C	6.36E+06 ± 5.4E+06	4.04E+05 ± 2.5E+05	1.99E+05 ± 1.8E+05	39.4 ± 21.5
	2C GFP	2.18E+06 ± 1.3E+06	1.40E+05 ± 4.6E+04	5.88E+04 ± 2.8E+04	41.3 ± 11.5
Spleen	2C	7.88E+07 ± 2.1E+07	6.30E+06 ± 2.1E+06	1.29E+05 ± 5.5E+04	2.0 ± 0.7
	2C GFP	8.02E+07 ± 2.2E+07	6.29E+06 ± 2.3E+06	1.29E+05 ± 1.1E+05	1.9 ± 1.1
Liver	2C	1.85E+06	6.23E+04	8.60E+03	13.7
	2C GFP	1.55E+06	3.40E+04	4.87E+03	12.8
MedLN	2C	9.23E+06 ± 9.0E+06	6.18E+05 ± 6.2E+05	1.99E+04 ± 2.3E+04	2.0 ± 1.7
	2C GFP	8.90E+06 ± 1.0E+07	8.67E+05 ± 1.2E+06	4.51E+04 ± 5.8E+04	3.3 ± 2.9
Lumbar LN	2C	1.58E+06	1.04E+05	2.25E+02	0.2
	2C GFP	2.85E+06	1.55E+05	2.83E+02	0.2

2C GFP cells remain in the lungs 30 dpi (Fig. 3a). These cells are CD8+ and CD44+ suggesting that they are memory T lymphocytes. Further analysis showed that they are also $CD62L^{low}$ (Fig. 3b). Interestingly, 10-20 times more 2C GFP effector memory cells are found in the lungs, compared to the spleen and lymph nodes (Table II). No GFP-expressing cells were found in livers 30 dpi (Fig. 3b and Table II).

(a)

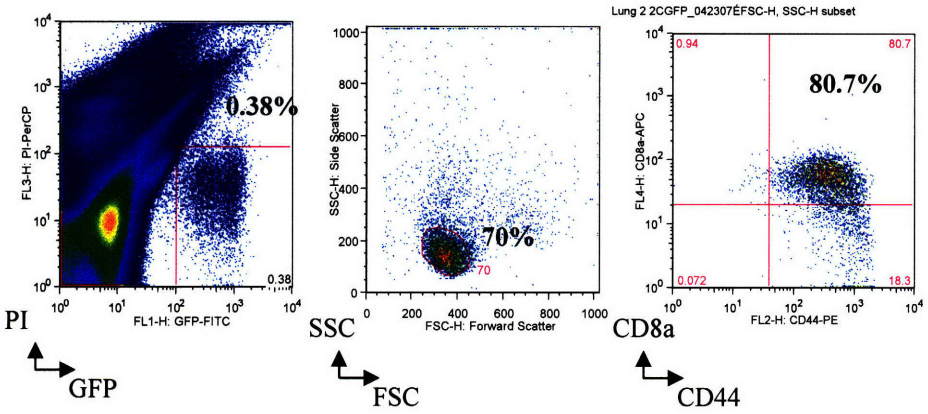

(b)

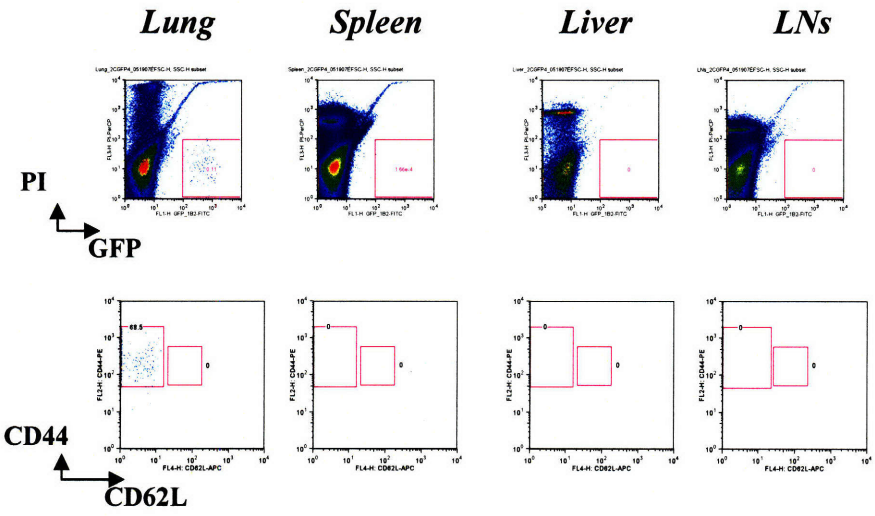

Fig. 3. 2C GFP memory cells persist in lung tissue up to 30 days after Influenza infection. **(a)** Representative plot showing GFP lymphocytes in lung tissue 30 days post 100 pfu WSN-SIY influenza infection. Cells were gated on PI versus GFP expression. Then, PI^{low} and GFP^{high} populations were gated on Side versus Forward scatter plots to eliminate residual erythrocytes and granulocytes. The lymphocyte population selected was analyzed for CD8a and CD44 expression. **(b)** Plot showing distribution of memory cells in different tissues for one representative 2C GFP recipient mouse infected with 100 pfu WSN-SIY influenza virus 30 days prior to flow cytometry analysis, as described in the methods section. The top row shows the gating for the live GFP cells using FlowJo software, after which CD44-PE and CD62L-APC populations were sorted (bottom row). Boundaries for the different populations were determined by comparison to corresponding tissue isolate from a naïve 2C RAG1-/- mouse. LNs include superficial cervical, mediastinal, mesenteric, inguinal and lumbar lymph nodes combined.

Table II. Average number of antigen-specific memory cells present in different tissues 30 days after influenza infection. All cells were isolated and stained with CD44-PE, CD62L-APC and PI for flow cytometry. In addition, 2C recipient mice cells were stained with Biotinylated 1B2 and Streptavidin-FITC. Analysis was performed using FlowJo software and Microsoft Excel. The standard deviation is given for groups that have 3-5 mice per group. Others have only 2 mice per group. LNs represents superficial cervical, mediastinal, mesenteric, inguinal and lumbar lymph nodes combined.

Tissue	Donor Cell Type	Total Number of Cells	Total # of GFP+/1B2+ CD44+ Cells	Total # of GFP+/1B2+ CD44+ CD62L^{Low} Cells
Lung	2C	4.75E+05	1.93E+04	1.39E+04
	2C GFP	1.15E+06 ± 9.0E+05	1.47E+03 ± 2.6E+03	170 ± 26
Spleen	2C	8.46E+07	6.25E+05	4.62E+05
	2C GFP	7.78E+07 ± 1.6E+07	89 ± 66	19 ± 33
Liver	2C	7.25E+05	1.62E+03	1.29E+03
	2C GFP	3.34+06 ± 3.35E+06	37 ± 73	0 ± 1
LNs	2C	1.90E+07	9.64E+04	4.26E+04
	2C GFP	1.63E+07 ± 4.5E+06	19 ± 26	8 ± 14

C.Discussion

Naïve T cells freshly isolated from 2C GFP and 2C donor mice were analyzed by flow cytometry before being transferred into B6 recipient mice. A distinct population of GFP-expressing cells (as shown in Fig. 1), ranging from approximately 60% to 82% of the CD8+ cell population were often observed. GFP-expression levels determined by the flow cytometer GFP gating did not appear to change from one T cell development stage -- naïve, effector (7 dpi) and memory (30 dpi) – to another.

Figure 2 and Table I show that 10^4-10^6 2C (antigen-specific) GFP-expressing T cells are found in the lung airways and parenchyma 7 days after WSN-SIY infection. This range is similar to values reported in literature [9, 12, 71]. Greater than 90% of these cells are both 1B2+ and CD8+ lymphocytes (Fig. 2a). These results suggest that tracking the GFP-expressing cells would be an appropriate model for identifying antigen-specific CD8+ T cells in lung tissue.

Figure 2b shows there is variability in cell numbers from mouse to mouse, but no significant difference was observed between 2C recipient and 2C GFP recipient mice 7 dpi. This variability may be due to differences in how many viral droplets actually enter the mouse lung during the intranasal infection process, and/or how many cells survive and actually enter the bloodstream during adoptive cell transfer.

Numbers of GFP+ CD8+ CD44+ cells 30 dpi are <6200 per mouse and range from 187 to 6162 cells per mouse (Table II). In addition to those mentioned above, differences in the cell numbers 30 dpi might reflect the variability in each mouse's immune response to intranasal influenza virus. Similar ranges of, 10^4-10^5, CD8+ CD44+ lymphocytes were found in all the tissues. However, 2C GFP memory cells predominantly resided in lung tissue, the primary site for influenza infection and CD8+ T cell response (Fig. 3). Less than 20% of all the GFP+ cells in the lung were $CD8a^{(-)}$ CD44+. Since our donor GFP-expressing cells were derived from mice in a RAG1-/- background, possibly the $CD8a^{(-)}$ CD44+ GFP-expressing cells are Natural Killer (NK) cells. CD44 is an integrin expressed on leukocytes and erythrocytes [4]. In the flow cytometry protocol, erythrocytes are depleted from the tissue homogenate using a red blood cell lysis buffer (see methods section). Also, this population is further removed during gating on the forward and side scatter subset using FlowJo software, so it is unlikely that erythrocytes contribute to this CD44+ population. Although future studies might warrant further investigation, our interest focused on being able to identify antigen-specific memory cells by fluorescence microscopy, and this group make up >80% of the GFP-expressing cell population.

Even though few 2C GFP memory cells were observed mainly in the lungs, both 2C and 2C GFP recipient mice appear to have similar numbers of CD8+ CD44+ memory lymphocytes in all tissues. The number of GFP-expressing cells in the lung are only about 12% of the CD8+

CD44+ memory cell population. This result suggests that an immune rejection of GFP might be occurring in the B6 recipient mice in synchrony with the response to influenza virus infection. It is possible that the vast majority of the non-GFP memory cells might be endogenous CD8+ T cells generated in response to antigenic GFP peptides [75]. Further studies would need to be performed to conclude if immune rejection against 2C GFP T cells occurs. Using GFP-tolerized recipient mice might be a valid approach for future studies if immune rejection is proven to be a conflicting issue. For the current purposes, these flow cytometry studies proved that effector memory 2C GFP cells are generated in the lung and are still present at least 30 days after influenza virus infection.

It is important to note that 2C GFP cells were found preferentially at the inflamed site -- the lungs -- of influenza infected mice. Lymphoid tissue such as spleens and lymph nodes had non-detectable or 10 times less 2C GFP memory cells than the lung, a non-lymphoid tissue (Table II). No 2C GFP cells were detected in the non-perfused liver, another non-lymphoid tissue (Table II). The fact that the liver was not perfused to remove lymphocytes in the blood before processing for flow cytometry, and that no 2C GFP cells were detected suggests that 2C GFP memory T cells may also not be circulating in the blood. There was no preference for lung tissue homing observed at day 7 after influenza infection (Fig. 2 and Table I) when cells are probably identifying and eliminating the source of the infection. The preferential distribution observed in the 30 dpi results strongly suggest that there are inherent differences in the ability of lymphoid and non-lymphoid tissue to sustain antigen-specific GFP+ memory cells. These results indicate that cellular interactions within non-lymphoid tissue may be important for cell-mediated immunity.

III.ANTIGEN-SPECIFIC T CELL DISTRIBUTION

A.Methods

Antibodies & Reagents: Sakura Finetek® Tissue-Tek O.C.T.™ embedding medium was purchased from VWR (USA). Biotinylated anti-CD31 (MEC13.3), biotinylated anti-CD11c, and anti-B220 conjugated to PE were purchased from BioLegend (San Diego, CA). Streptavidin conjugated Alexa Fluor 647 and Hoechst 33342 dye were acquired from Invitrogen Molecular Probes (USA).

Tissue Processing and Sectioning: Each tissue of interest was extracted from mice, one after another, sacrificed by carbon dioxide (CO_2) asphyxiation followed by spraying with 70% ethanol or quatricide. In the case of the lung, intratracheal inflation with 50% Tissue-Tek O.C.T.™ embedding medium in 1x PBS, was performed prior to removing the lungs. The extracted tissue was immediately transferred into tubes containing RPMI complete on ice. Upon completion of the harvesting process, each lung lobe or single organ was transferred into appropriately labeled embedding molds. Tissue-Tek O.C.T.™ embedding medium was added to each mold containing tissue. The molds were immediately kept on dry ice sprayed with 70% ethanol for rapid freezing and kept on dry ice for at least 15 min. Embedded tissue blocks were stored at -80°C until cryosectioning (by the MIT CCR histology facility). Frozen sections were also stored at -80°C before immunostaining and microscopy analysis.

Immunofluorescence Staining: Frozen sections mounted on microscope slides were retrieved from -80 °C and fixed on ice in a 4 °C cold room with cold acetone (Sigma-Aldrich) which had been kept at -20 °C for 5-10 min. Then the tissue slides were rinsed 1x with BSA-containing

Wash buffer (0.05% glycine and 0.75% BSA in 1x PBS). BSA (Bovine serum albumin) helps to reduce non-specific binding. A region around the tissue was marked using a Liquid Blocker Super Pap Pen (Daido Sangyo Co. Ltd., Japan). Two hundred microliters each of FCS-Blocking buffer (10% FCS and 0.1% sodium azide in 1x PBS) was added to each tissue specimen and left to incubate at room temperature (RT) for 1 hr in a humid chamber. Following incubation, non-specific streptavidin binding was reduced by using a Streptavidin-Biotin blocking kit (Vector Labs) according to the manufacturer's instructions. Then 200 µl per specimen of supernatant from the centrifuged primary biotinylated antibody 1:100 dilution (~5 µg) in FCS-blocking media was added. The incubation proceeded for 1 hr at RT in the humid chamber. Specimens were washed twice, following incubation, with 200 µl each of the BSA-containing Wash buffer for 5 min each time. Then 200 µl per specimen of supernatant from the centrifuged secondary cocktail in FCS-blocking media was added. The secondary cocktail consisted of the secondary antibody Streptavidin-Alexa Fluor 647 (Invitrogen, 1:100), Hoechst dye (Invitrogen, 1:1000), and where indicated, B220-PE antibody (1:100) in FCS-blocking media. The tissue sections were incubated for another hour at RT in a humid chamber covered with foil paper. After incubation, each specimen was washed thrice with BSA-containing Wash buffer. Each wash lasted 5 min. The slides were kept covered in foil during washes. Slides were "air-dried" for at least 20 min in dry chambers, covered loosely with foil paper, to remove excess moisture before adding pre-warmed ProLong Gold (Invitrogen), according to manufacturer's instructions. Slides were viewed by fluorescence microscopy 24 hr after curing at RT wrapped up in foil paper.

Tissue Microscopy and Analysis: Tissue sections were viewed using a Zeiss Axiovert 200M microscope equipped with an 84000 series quad filter set having single band pass excitation

filters for DAPI/FITC/TRITC/Cy5, and a Hamamatsu ORCA-AG camera. Images were acquired using an A-Plan 10x/0.25 Ph1 and LD Plan Neofluar 40x/0.6 Ph objective lenses. Further image analysis was performed using Imaris software.

B.Results

1. T Cell Distribution in Lung

Lymphocytes, polymorphonuclear cells and macrophages were observed in H&E lung sections of mice that had been adoptively transferred with 2C or 2C GFP T cells and infected with 100 pfu WSN-SIY influenza virus (Fig. 4a). Severe vasculitis and gross inflammatory infiltrates in all areas of the lung were distinct hallmarks of infection. By fluorescence microscopy, 2C GFP cells were found in vessels, bronchioles and alveolar spaces (Fig. 4b) particularly in lower lung lobes.

In mice transferred with 2C GFP cells, GFP cells were observed in peribronchiolar and stromal areas of the lung 31 dpi (Fig. 5). Less than 2 cells were identified per 120-150 μm total section of lung. More often, no GFP cells were observed in these blocks. There appeared to be no preference for either lower or upper lung lobes.

(a)

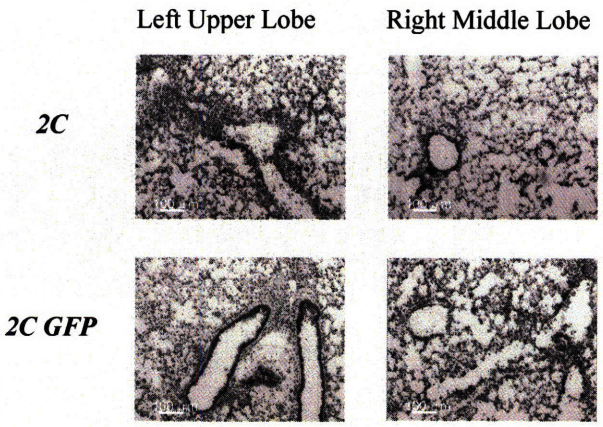

(b)

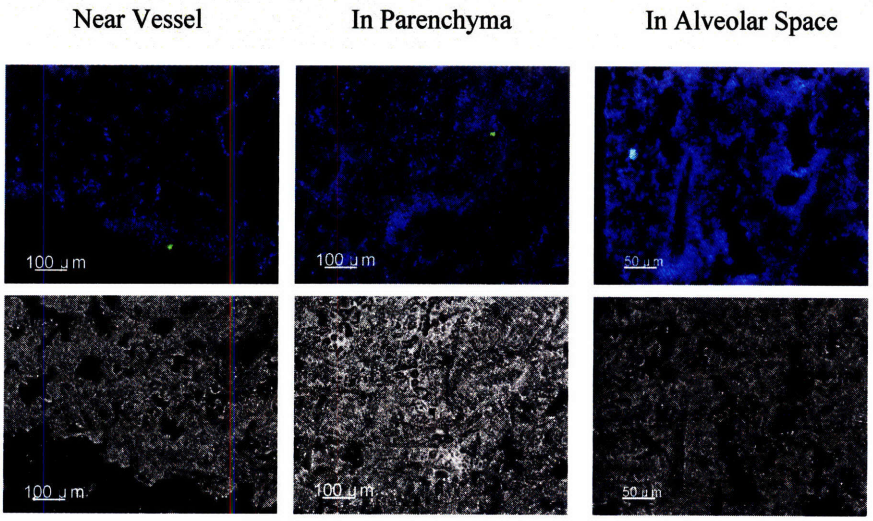

Fig. 4. 2C GFP recipient mice exhibit similar lung pathology to 2C recipient mice 7 days after influenza virus infection. **(a)** A representative plot of Hematoxylin and Eosin stained frozen 10-µm lung sections. The left panel shows more severe vasculitis in the left lower lobes compared to the right middle lobes. **(b)** 2C GFP cells found near vessel (left), in lung parenchyma (middle) and in alveolar spaces (right) of cold acetone-fixed 10-µm Tissue-Tek O.C.T. embedded frozen sections. Images were acquired using a Zeiss Axiovert 200M microscope and analyzed with Imaris software as described in the methods section. Nuclei stained with Hoechst dye are pseudo-colored blue, 2C GFP cells colored green, and anti-CD31 labeled endothelial vessels in red. Light images are in gray (bottom panels).

(a)

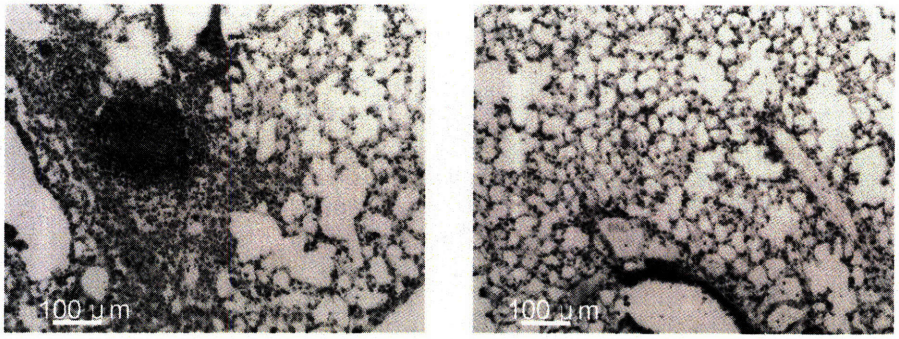

(b)

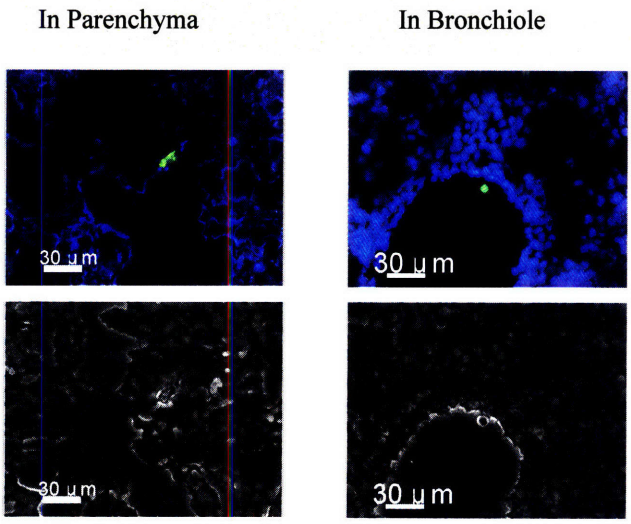

Fig. 5. Distribution of antigen-specific memory T cells after influenza infection. **(a)** Representative Hematoxylin and Eosin stained frozen lung sections from 2C GFP recipient mice infected with 100 pfu of WSN-SIY influenza virus 31 days post-infection. The sections are 15-µm thick. Left image shows lymphoid-appearing nodule and right image illustrates clear alveolar spaces typically observed in all lobes **(b)** 2C GFP-expressing cells (green) are found in the lung parenchyma and peribronchiolar areas of cold-acetone fixed 15-µm frozen sections. Nuclei were stained with Hoechst dye (blue). Images were acquired with a Zeiss Axiovert 200M and Hamamatsu ORCA-AG camera using AxioVision software. Further processing was performed with Imaris software.

2. Investigation of T Cell – Dendritic Cell Interactions

Frozen lung tissue sections were stained with anti-CD11c to identify dendritic cells by immunofluorescence. GFP T cells were rarely seen in the same view as dendritic cells. The closest association between a GFP T cell and a dendritic cell is about 30-µm apart (Fig. 6 lower right image). No T or B cell clusters were observed.

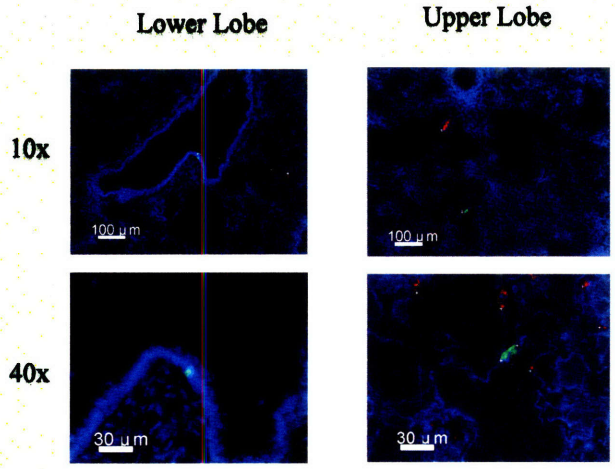

Fig. 6. 2C GFP memory T cells do not appear to colocalize with resident lung dendritic cells. Plot shows the closest associations observed between 2C GFP memory cells (green) 31 days after 100 pfu WSN-SIY influenza infection. 15-µm lung frozen sections were cold acetone-fixed, stained with biotinylated anti-CD11c, Streptavidin-Alexa Fluor 647 (red), anti-B220-PE, and Hoechst dye (blue), and mounted with ProLong Gold. Images were acquired with a Zeiss Axiovert 200M and Hamamatsu ORCA-AG camera using AxioVision software. Further processing was performed with Imaris software.

C.Discussion

Antigen-specific effector CD8+ T cells are found widely distributed in the lung airways and vessels seven days after influenza infection. Hematoxylin and Eosin (H&E) stained slides revealed that 2C GFP recipient mice have similar lung pathology to 2C recipient mice (Fig. 4a). Inflammatory cells – lymphocytes, polymorphonuclear cells, and macrophages – can be found in the alveolar spaces, vasculature and bronchioles (Fig. 4), completely defacing the lung morphology. More severe vasculitis is observed in the lower lobes compared to upper and middle lung lobes. These images are in agreement with previously published results [23-25].

In frozen sections of lungs, 2C GFP effector cells were identified by their GFP signal above the background fluorescence and a diameter of about 10-15 µm. Occasionally, GFP nuclei-stained cells about 30-um diameter were seen. These cells had bleb-like structures that

suggest these were dying T cells (data not shown). It was determined from *in vitro* imaging of isolated lymphocytes that dead cells do not express GFP (data not shown). Rough estimates showed that only about 530 viable GFP cells would have been detected by fluorescence microscopy in 7 dpi lung frozen sections. This is about 1% of the population of GFP cells estimated by flow cytometry studies. It is possible that fluorescence signal from cells that overlap with the yellow-green autofluorescence are missed, and might have been removed whilst setting lower thresholds based on background fluorescence from 2C recipient and influenza infected mice. Of note, yellow-green autofluorescence observed in the lung tissue was reduced by the initial 5-10 min cold acetone fixation. Cold 2 or 4% paraformaldehyde fixation up to 1 hr did not appear to reduce the yellow-green autofluorescence in lung specimens. Both methods of fixation maintained the tissue architecture when compared to unfixed sections, and neither one appeared to reduce orange-red autofluorescence.

Hematoxylin-and-eosin stained sections 31 dpi showed clearer alveolar spaces and airways when compared to H&E sections from 7 dpi (see Fig 4a and 5a). This reduced numbers of inflammatory infiltrates 31 dpi indicates that surviving mice had recovered from the infection. Viral titers from studies by different groups have shown that influenza virus levels become non-detectable by 15 days after acute infection in an immunocompetent model, and the lung architecture is restored [23, 26, 27]. In lung frozen sections, an estimate of thirty 2C GFP cells would have been observed per mouse. Cells were seen in bronchioles and in the lung parenchyma 31 days after influenza infection sparsely distributed within upper and lower lung lobes. Based on flow cytometry studies, these cells would be effector memory, CD8+ CD44+ $CD62L^{low}$ 2C TCR cells.

At this low dose (100 pfu) of influenza virus infection, induced bronchus-associated lymphoid tissue (iBALT) would not be expected. Although lymphoid-appearing nodules near vessels and bronchioles were observed in most of the lung lobes, staining with anti-B220 did not show any B cell clusters in close proximity to GFP-expressing T cells.

From these images, it appears that the lymphocytes enter the lungs via the vasculature. The process might involve burrowing channels through vessels; similar to the process of diapedesis described for high endothelial vessels in lymph nodes [17]. This process might explain the severe vasculitis observed in the lung lobes. As the virus is cleared, contraction of the antigen-specific cells occurs and the airway passages are cleared [23, 26, 27]. Memory T cells then reside in stroma-rich areas for sustenance [23, 26, 27].

Lung stroma cells consist of fibroblasts which may be a source of IL-15/Rα, a cytokine proven to be necessary for memory CD8+ T cell proliferation and maintenance [43-48]. The lung also has epithelial cells and dendritic cells that have also been identified as sources of IL-15. The closest association between a GFP T cell and a dendritic cell identified by CD11c staining was about 30-μm apart. Dendritic cells are found in airways as well as in the lung parenchyma [76]. Based on the number of $CD11c^+$ stained cells (Fig. 6), there are about 5×10^6 dendritic cells in the lung. This estimate is four times less than the number obtained from flow cytometry studies [77]. Although this number suggests dendritic cells are abundant in the lungs, most GFP T cells in the lung parenchyma did not colocalize with dendritic cells. By inflating the lungs with embedding media before the tissue is sectioned, it possible that associations in the airways were disrupted. These studies focused on cells in the lung parenchyma which are not dislodged by inflation [78]. Amongst the high intensity GFP cells easily detected by microscopy, there was no indication that antigen-specific T cells and dendritic cells routinely form stable contacts which

would have been detected by overlap in GFP and Alexa Fluor 647 signals. Further studies need to be carried out in order to identify whether antigen-specific cells preferentially reside near other known IL-15 secreting cell types in the lung.

IV.SUMMARY & CONCLUSION

In this study, we show that antigen-specific 2C GFP effector memory CD8+ T cells are generated in B6 recipient mice 30-32 days after influenza virus infection. In agreement with previously published studies [27], CD8+ memory T cells against influenza virus preferentially reside in peribronchiolar areas. Both 2C and 2C GFP recipient mice gross inflammation and severe vasculitis in lungs 7 days post-infection. Lower lung lobes appear to be more adversely affected by the infection and immune response than upper lobes at this time point.

About 3-4 weeks later, the alveolar spaces appear to be completely restored. Some regions showed lymphoid-appearing nodules 31 dpi. However, no B and T cell clusters suggesting induced BALT were identified by immunofluorescence staining. Antigen-specific GFP cells preferentially remained in the lung tissue and were almost in lymphoid and other non-lymphoid tissues. This preference was not observed in the 2C non-GFP recipient mice. Further analysis showed no colocalization between 2C GFP T cells and dendritic cells in the lung parenchyma. More work is needed to determine what structural elements in non-lymphoid tissue influence cell-mediated immunity.

V.BIBLIOGRAPHY

(1) Doherty, P. C.; Turner, S. J.; Webby, R. G.; Thomas, P. G. Influenza and the Challenge for Immunology. *Nat. Immunol.* **2006**, *7*, 449-455.

(2) Yewdell, J. W.; Haeryfar, S. M. Understanding Presentation of Viral Antigens to CD8+ T Cells in Vivo: The Key to Rational Vaccine Design. *Annu. Rev. Immunol.* **2005**, *23*, 651-682.

(3) Haeryfar, S. M.; DiPaolo, R. J.; Tscharke, D. C.; Bennink, J. R.; Yewdell, J. W. Regulatory T Cells Suppress CD8+ T Cell Responses Induced by Direct Priming and Cross-Priming and Moderate Immunodominance Disparities. *J. Immunol.* **2005**, *174*, 3344-3351.

(4) Abbas, A. K.; Lichtman, A. H.; Pober, J. S. In *Cellular and molecular immunology;* W.B. Saunders: Philadelphia, 2000; , pp 553.

(5) Ali, S.; Ahmad, M.; Lynam, J.; Rees, R. C.; Brown, N. Trafficking of Tumor Peptide-Specific Cytotoxic T Lymphocytes into the Tumor Microcirculation. *Int. J. Cancer* **2004**, *110*, 239-244.

(6) Kircher, M. F.; Allport, J. R.; Graves, E. E.; Love, V.; Josephson, L.; Lichtman, A. H.; Weissleder, R. In Vivo High Resolution Three-Dimensional Imaging of Antigen-Specific Cytotoxic T-Lymphocyte Trafficking to Tumors. *Cancer Res.* **2003**, *63*, 6838-6846.

(7) Lawrence, C. W.; Braciale, T. J. Activation, Differentiation, and Migration of Naive Virus-Specific CD8+ T Cells during Pulmonary Influenza Virus Infection. *J. Immunol.* **2004**, *173*, 1209-1218.

(8) Mempel, T. R.; Henrickson, S. E.; Von Andrian, U. H. T-Cell Priming by Dendritic Cells in Lymph Nodes Occurs in Three Distinct Phases. *Nature* **2004**, *427*, 154-159.

(9) Hugues, S.; Fetler, L.; Bonifaz, L.; Helft, J.; Amblard, F.; Amigorena, S. Distinct T Cell Dynamics in Lymph Nodes during the Induction of Tolerance and Immunity. *Nat. Immunol.* **2004**, *5*, 1235-1242.

(10) Lefrancois, L.; Puddington, L. Intestinal and Pulmonary Mucosal T Cells: Local Heroes Fight to Maintain the Status Quo. *Annu. Rev. Immunol.* **2006**, *24*, 681-704.

(11) Lindquist, R. L.; Shakhar, G.; Dudziak, D.; Wardemann, H.; Eisenreich, T.; Dustin, M. L.; Nussenzweig, M. C. Visualizing Dendritic Cell Networks in Vivo. *Nat. Immunol.* **2004**, *5*, 1243-1250.

(12) Bousso, P.; Robey, E. Dynamics of CD8+ T Cell Priming by Dendritic Cells in Intact Lymph Nodes. *Nat. Immunol.* **2003**, *4*, 579-585.

(13) Miller, M. J.; Wei, S. H.; Cahalan, M. D.; Parker, I. Autonomous T Cell Trafficking Examined in Vivo with Intravital Two-Photon Microscopy. *Proc. Natl. Acad. Sci. U. S. A.* **2003**, *100*, 2604-2609.

(14) Stoll, S.; Delon, J.; Brotz, T. M.; Germain, R. N. Dynamic Imaging of T Cell-Dendritic Cell Interactions in Lymph Nodes. *Science* **2002**, *296*, 1873-1876.

(15) Miller, M. J.; Safrina, O.; Parker, I.; Cahalan, M. D. Imaging the Single Cell Dynamics of CD4+ T Cell Activation by Dendritic Cells in Lymph Nodes. *J. Exp. Med.* **2004**, *200*, 847-856.

(16) Masopust, D.; Vezys, V.; Usherwood, E. J.; Cauley, L. S.; Olson, S.; Marzo, A. L.; Ward, R. L.; Woodland, D. L.; Lefrancois, L. Activated Primary and Memory CD8 T Cells Migrate to Nonlymphoid Tissues Regardless of Site of Activation Or Tissue of Origin. *J. Immunol.* **2004**, *172*, 4875-4882.

(17) Halin, C.; Rodrigo Mora, J.; Sumen, C.; von Andrian, U. H. In Vivo Imaging of Lymphocyte Trafficking. *Annu. Rev. Cell Dev. Biol.* **2005**, *21*, 581-603.

(18) Lamb, R. A.; Krug, R. M. In *Orthomyxoviridae: the viruses and their replication;* Knipe, D. M., Howley, P. M., Eds.; Lippincott Williams and Wilkins: Philadelphia, 2001; pp 1487-1531.

(19) Legge, K. L.; Braciale, T. J. Lymph Node Dendritic Cells Control CD8+ T Cell Responses through Regulated FasL Expression. *Immunity* **2005**, *23*, 649-659.

(20) Johnson, B. J.; Costelloe, E. O.; Fitzpatrick, D. R.; Haanen, J. B.; Schumacher, T. N.; Brown, L. E.; Kelso, A. Single-Cell Perforin and Granzyme Expression Reveals the Anatomical Localization of Effector CD8+ T Cells in Influenza Virus-Infected Mice. *Proc. Natl. Acad. Sci. U. S. A.* **2003**, *100*, 2657-2662.

(21) Shinya, K.; Kawaoka, Y. Influenza Virus Receptors in the Human Airway. *Uirusu* **2006**, *56*, 85-89.

(22) Russell, J. H.; Ley, T. J. Lymphocyte-Mediated Cytotoxicity. *Annu. Rev. Immunol.* **2002**, *20*, 323-370.

(23) Chen, H. D.; Fraire, A. E.; Joris, I.; Welsh, R. M.; Selin, L. K. Specific History of Heterologous Virus Infections Determines Anti-Viral Immunity and Immunopathology in the Lung. *Am. J. Pathol.* **2003**, *163*, 1341-1355.

(24) Mackenzie, C. D.; Taylor, P. M.; Askonas, B. A. Rapid Recovery of Lung Histology Correlates with Clearance of Influenza Virus by Specific CD8+ Cytotoxic T Cells. *Immunology* **1989**, *67*, 375-381.

(25) Thatte, J.; Dabak, V.; Williams, M. B.; Braciale, T. J.; Ley, K. LFA-1 is Required for Retention of Effector CD8 T Cells in Mouse Lungs. *Blood* **2003**, *101*, 4916-4922.

(26) Wiley, J. A.; Hogan, R. J.; Woodland, D. L.; Harmsen, A. G. Antigen-Specific CD8(+) T Cells Persist in the Upper Respiratory Tract Following Influenza Virus Infection. *J. Immunol.* **2001**, *167*, 3293-3299.

(27) Hogan, R. J.; Usherwood, E. J.; Zhong, W.; Roberts, A. A.; Dutton, R. W.; Harmsen, A. G.; Woodland, D. L. Activated Antigen-Specific CD8+ T Cells Persist in the Lungs Following Recovery from Respiratory Virus Infections. *J. Immunol.* **2001**, *166*, 1813-1822.

(28) Shen, C. H.; Ge, Q.; Talay, O.; Eisen, H. N.; Garcia-Sastre, A.; Chen, J. Loss of Interleukin (IL)-7 and IL-15 Receptors is Associated with Disappearance of Memory T Cells from Respiratory Tract After Influenza Infection. *Manuscript* **2007**.

(29) Sallusto, F.; Lenig, D.; Forster, R.; Lipp, M.; Lanzavecchia, A. Two Subsets of Memory T Lymphocytes with Distinct Homing Potentials and Effector Functions. *Nature* **1999**, *401*, 708-712.

(30) Roberts, A. D.; Woodland, D. L. Cutting Edge: Effector Memory CD8+ T Cells Play a Prominent Role in Recall Responses to Secondary Viral Infection in the Lung. *J. Immunol.* **2004**, *172*, 6533-6537.

(31) Welsh, R. M.; Selin, L. K.; Szomolanyi-Tsuda, E. Immunological Memory to Viral Infections. *Annu. Rev. Immunol.* **2004**, *22*, 711-743.

(32) Masopust, D.; Vezys, V.; Marzo, A. L.; Lefrancois, L. Preferential Localization of Effector Memory Cells in Nonlymphoid Tissue. *Science* **2001**, *291*, 2413-2417.

(33) de Bree, G. J.; van Leeuwen, E. M.; Out, T. A.; Jansen, H. M.; Jonkers, R. E.; van Lier, R. A. Selective Accumulation of Differentiated CD8+ T Cells Specific for Respiratory Viruses in the Human Lung. *J. Exp. Med.* **2005**, *202*, 1433-1442.

(34) Ely, K. H.; Cauley, L. S.; Roberts, A. D.; Brennan, J. W.; Cookenham, T.; Woodland, D. L. Nonspecific Recruitment of Memory CD8+ T Cells to the Lung Airways during Respiratory Virus Infections. *J. Immunol.* **2003**, *170*, 1423-1429.

(35) Barber, D. L.; Wherry, E. J.; Ahmed, R. Cutting Edge: Rapid in Vivo Killing by Memory CD8 T Cells. *J. Immunol.* **2003**, *171*, 27-31.

(36) Liang, S.; Mozdzanowska, K.; Palladino, G.; Gerhard, W. Heterosubtypic Immunity to Influenza Type A Virus in Mice. Effector Mechanisms and their Longevity. *J. Immunol.* **1994**, *152*, 1653-1661.

(37) Ely, K. H.; Cookenham, T.; Roberts, A. D.; Woodland, D. L. Memory T Cell Populations in the Lung Airways are Maintained by Continual Recruitment. *J. Immunol.* **2006**, *176*, 537-543.

(38) Lefrancois, L. Development, Trafficking, and Function of Memory T-Cell Subsets. *Immunol. Rev.* **2006**, *211*, 93-103.

(39) Surh, C. D.; Boyman, O.; Purton, J. F.; Sprent, J. Homeostasis of Memory T Cells. *Immunol. Rev.* **2006**, *211*, 154-163.

(40) Weninger, W.; Crowley, M. A.; Manjunath, N.; von Andrian, U. H. Migratory Properties of Naive, Effector, and Memory CD8(+) T Cells. *J. Exp. Med.* **2001**, *194*, 953-966.

(41) Stoklasek, T. A.; Schluns, K. S.; Lefrancois, L. Combined IL-15/IL-15Ralpha Immunotherapy Maximizes IL-15 Activity in Vivo. *J. Immunol.* **2006**, *177*, 6072-6080.

(42) Becker, T. C.; Coley, S. M.; Wherry, E. J.; Ahmed, R. Bone Marrow is a Preferred Site for Homeostatic Proliferation of Memory CD8 T Cells. *J. Immunol.* **2005**, *174*, 1269-1273.

(43) Lodolce, J. P.; Boone, D. L.; Chai, S.; Swain, R. E.; Dassopoulos, T.; Trettin, S.; Ma, A. IL-15 Receptor Maintains Lymphoid Homeostasis by Supporting Lymphocyte Homing and Proliferation. *Immunity* **1998**, *9*, 669-676.

(44) Kennedy, M. K., et al Reversible Defects in Natural Killer and Memory CD8 T Cell Lineages in Interleukin 15-Deficient Mice. *J. Exp. Med.* **2000**, *191*, 771-780.

(45) Becker, T. C.; Wherry, E. J.; Boone, D.; Murali-Krishna, K.; Antia, R.; Ma, A.; Ahmed, R. Interleukin 15 is Required for Proliferative Renewal of Virus-Specific Memory CD8 T Cells. *J. Exp. Med.* **2002**, *195*, 1541-1548.

(46) Schluns, K. S.; Williams, K.; Ma, A.; Zheng, X. X.; Lefrancois, L. Cutting Edge: Requirement for IL-15 in the Generation of Primary and Memory Antigen-Specific CD8 T Cells. *J. Immunol.* **2002**, *168*, 4827-4831.

(47) Judge, A. D.; Zhang, X.; Fujii, H.; Surh, C. D.; Sprent, J. Interleukin 15 Controls both Proliferation and Survival of a Subset of Memory-Phenotype CD8(+) T Cells. *J. Exp. Med.* **2002**, *196*, 935-946.

(48) Wu, T. S.; Lee, J. M.; Lai, Y. G.; Hsu, J. C.; Tsai, C. Y.; Lee, Y. H.; Liao, N. S. Reduced Expression of Bcl-2 in CD8+ T Cells Deficient in the IL-15 Receptor Alpha-Chain. *J. Immunol.* **2002**, *168*, 705-712.

(49) Liu, Z.; Geboes, K.; Colpaert, S.; D'Haens, G. R.; Rutgeerts, P.; Ceuppens, J. L. IL-15 is Highly Expressed in Inflammatory Bowel Disease and Regulates Local T Cell-Dependent Cytokine Production. *J. Immunol.* **2000**, *164*, 3608-3615.

(50) Muro, S.; Taha, R.; Tsicopoulos, A.; Olivenstein, R.; Tonnel, A. B.; Christodoulopoulos, P.; Wallaert, B.; Hamid, Q. Expression of IL-15 in Inflammatory Pulmonary Diseases. *J. Allergy Clin. Immunol.* **2001**, *108*, 970-975.

(51) Klonowski, K. D.; Marzo, A. L.; Williams, K. J.; Lee, S. J.; Pham, Q. M.; Lefrancois, L. CD8 T Cell Recall Responses are Regulated by the Tissue Tropism of the Memory Cell and Pathogen. *J. Immunol.* **2006**, *177*, 6738-6746.

(52) Moyron-Quiroz, J. E.; Rangel-Moreno, J.; Hartson, L.; Kusser, K.; Tighe, M. P.; Klonowski, K. D.; Lefrancois, L.; Cauley, L. S.; Harmsen, A. G.; Lund, F. E.; Randall, T. D. Persistence and Responsiveness of Immunologic Memory in the Absence of Secondary Lymphoid Organs. *Immunity* **2006**, *25*, 643-654.

(53) Moyron-Quiroz, J. E.; Rangel-Moreno, J.; Kusser, K.; Hartson, L.; Sprague, F.; Goodrich, S.; Woodland, D. L.; Lund, F. E.; Randall, T. D. Role of Inducible Bronchus Associated Lymphoid Tissue (iBALT) in Respiratory Immunity. *Nat. Med.* **2004**, *10*, 927-934.

(54) Hikono, H.; Kohlmeier, J. E.; Ely, K. H.; Scott, I.; Roberts, A. D.; Blackman, M. A.; Woodland, D. L. T-Cell Memory and Recall Responses to Respiratory Virus Infections. *Immunol. Rev.* **2006**, *211*, 119-132.

(55) Hendriks, J.; Xiao, Y.; Rossen, J. W.; van der Sluijs, K. F.; Sugamura, K.; Ishii, N.; Borst, J. During Viral Infection of the Respiratory Tract, CD27, 4-1BB, and OX40 Collectively Determine Formation of CD8+ Memory T Cells and their Capacity for Secondary Expansion. *J. Immunol.* **2005**, *175*, 1665-1676.

(56) Kelley, J.; Chrin, L.; Coflesky, J. T.; Evans, J. N. Localization of Collagen in the Rat Lung: Biochemical Quantitation of Types I and III Collagen in Small Airways, Vessels, and Parenchyma. *Lung* **1989**, *167*, 313-322.

(57) Gil, J.; Martinez-Hernandez, A. The Connective Tissue of the Rat Lung: Electron Immunohistochemical Studies. *J. Histochem. Cytochem.* **1984**, *32*, 230-238.

(58) Amenta, P. S.; Gil, J.; Martinez-Hernandez, A. Connective Tissue of Rat Lung. II: Ultrastructural Localization of Collagen Types III, IV, and VI. *J. Histochem. Cytochem.* **1988**, *36*, 1167-1173.

(59) Kim, J. K.; Xu, Y.; Xu, X.; Keene, D. R.; Gurusiddappa, S.; Liang, X.; Wary, K. K.; Hook, M. A Novel Binding Site in Collagen Type III for Integrins alpha1beta1 and alpha2beta1. *J. Biol. Chem.* **2005**, *280*, 32512-32520.

(60) Ray, S. J.; Franki, S. N.; Pierce, R. H.; Dimitrova, S.; Koteliansky, V.; Sprague, A. G.; Doherty, P. C.; de Fougerolles, A. R.; Topham, D. J. The Collagen Binding alpha1beta1 Integrin VLA-1 Regulates CD8 T Cell-Mediated Immune Protection Against Heterologous Influenza Infection. *Immunity* **2004**, *20*, 167-179.

(61) Rappl, G.; Kapsokefalou, A.; Heuser, C.; Rossler, M.; Ugurel, S.; Tilgen, W.; Reinhold, U.; Abken, H. Dermal Fibroblasts Sustain Proliferation of Activated T Cells Via Membrane-Bound Interleukin-15 upon Long-Term Stimulation with Tumor Necrosis Factor-Alpha. *J. Invest. Dermatol.* **2001**, *116*, 102-109.

(62) Briard, D.; Brouty-Boye, D.; Azzarone, B.; Jasmin, C. Fibroblasts from Human Spleen Regulate NK Cell Differentiation from Blood CD34(+) Progenitors Via Cell Surface IL-15. *J. Immunol.* **2002**, *168*, 4326-4332.

(63) Handisurya, A.; Steiner, G. E.; Stix, U.; Ecker, R. C.; Pfaffeneder-Mantai, S.; Langer, D.; Kramer, G.; Memaran-Dadgar, N.; Marberger, M. Differential Expression of Interleukin-15, a Pro-Inflammatory Cytokine and T-Cell Growth Factor, and its Receptor in Human Prostate. *Prostate* **2001**, *49*, 251-262.

(64) Mattei, F.; Schiavoni, G.; Belardelli, F.; Tough, D. F. IL-15 is Expressed by Dendritic Cells in Response to Type I IFN, Double-Stranded RNA, Or Lipopolysaccharide and Promotes Dendritic Cell Activation. *J. Immunol.* **2001**, *167*, 1179-1187.

(65) Doherty, T. M.; Seder, R. A.; Sher, A. Induction and Regulation of IL-15 Expression in Murine Macrophages. *J. Immunol.* **1996**, *156*, 735-741.

(66) Pelletier, M.; Girard, D. Interleukin-15 Increases Neutrophil Adhesion Onto Human Respiratory Epithelial A549 Cells and Attracts Neutrophils in Vivo. *Clin. Exp. Immunol.* **2005**, *141*, 315-325.

(67) Sandau, M. M.; Schluns, K. S.; Lefrancois, L.; Jameson, S. C. Cutting Edge: Transpresentation of IL-15 by Bone Marrow-Derived Cells Necessitates Expression of IL-15 and IL-15R Alpha by the Same Cells. *J. Immunol.* **2004**, *173*, 6537-6541.

(68) Dubois, S.; Mariner, J.; Waldmann, T. A.; Tagaya, Y. IL-15Ralpha Recycles and Presents IL-15 in Trans to Neighboring Cells. *Immunity* **2002**, *17*, 537-547.

(69) Schluns, K. S.; Stoklasek, T.; Lefrancois, L. The Roles of Interleukin-15 Receptor Alpha: Trans-Presentation, Receptor Component, Or both? *Int. J. Biochem. Cell Biol.* **2005**, *37*, 1567-1571.

(70) Sato, N.; Patel, H. J.; Waldmann, T. A.; Tagaya, Y. The IL-15/IL-15Ralpha on Cell Surfaces Enables Sustained IL-15 Activity and Contributes to the Long Survival of CD8 Memory T Cells. *Proc. Natl. Acad. Sci. U. S. A.* **2007**, *104*, 588-593.

(71) McGavern, D. B.; Christen, U.; Oldstone, M. B. Molecular Anatomy of Antigen-Specific CD8(+) T Cell Engagement and Synapse Formation in Vivo. *Nat. Immunol.* **2002**, *3*, 918-925.

(72) Chen, J.; Eisen, H. N.; Kranz, D. M. A Model T-Cell Receptor System for Studying Memory T-Cell Development. *Microbes Infect.* **2003**, *5*, 233-240.

(73) Okabe, M.; Ikawa, M.; Kominami, K.; Nakanishi, T.; Nishimune, Y. 'Green Mice' as a Source of Ubiquitous Green Cells. *FEBS Lett.* **1997**, *407*, 313-319.

(74) Fodor, E.; Devenish, L.; Engelhardt, O. G.; Palese, P.; Brownlee, G. G.; Garcia-Sastre, A. Rescue of Influenza A Virus from Recombinant DNA. *J. Virol.* **1999**, *73*, 9679-9682.

(75) Stripecke, R.; Carmen Villacres, M.; Skelton, D.; Satake, N.; Halene, S.; Kohn, D. Immune Response to Green Fluorescent Protein: Implications for Gene Therapy. *Gene Ther.* **1999**, *6*, 1305-1312.

(76) de Heer, H. J.; Hammad, H.; Kool, M.; Lambrecht, B. N. Dendritic Cell Subsets and Immune Regulation in the Lung. *Semin. Immunol.* **2005**, *17*, 295-303.

(77) Roghanian, A.; Williams, S. E.; Sheldrake, T. A.; Brown, T. I.; Oberheim, K.; Xing, Z.; Howie, S. E.; Sallenave, J. M. The antimicrobial/elastase Inhibitor Elafin Regulates Lung Dendritic Cells and Adaptive Immunity. *Am. J. Respir. Cell Mol. Biol.* **2006**, *34*, 634-642.

(78) Schmiedl, A.; Tschernig, T.; Luhrmann, A.; Pabst, R. Leukocyte Infiltration of the Periarterial Space of the Lung After Allergen Provocation in a Rat Asthma Model. *Pathobiology* **2005**, *72*, 308-315.

VI.ABBREVIATIONS LIST

2C	2C T Cell Receptor cells
2C GFP	GFP-expressing 2C T Cell Receptor cells
APC	allophycocyanin
BALT	bronchus-associated lymphoid tissue
BSA	bovine serum albumin
dpi	days post-infection
FACS	fluorescence-activated cell sorting
FCS	fetal calf serum
FITC	fluorescein isothiocyanate
GFP	green fluorescent protein
H&E	hematoxylin and eosin
HA	hemagglutinin
LN	lymph node
NA	neuraminidase
NK	natural killer (cells)
PBS	phosphate buffered saline
PE	phycoerythrin
PI	propidium iodide
RAG	recombination activating gene
SIY	SIYRYYGL (Ser-Ile-Tyr-Arg-Tyr-Tyr-Gly-Leu) peptide sequence encoded onto the WSN influenza virus neuraminidase stalk
TCR	T cell receptor

VII.ACKNOWLEDGEMENTS

I would like to thank my advisors, Paul Matsudaira and Jianzhu Chen for their continued support as I developed and worked on this project. Special thanks to all members of the Matsudaira and Chen labs for teaching me techniques, sharing reagents, and providing helpful discussions along the way. In particular, this project would not have been possible without advice from Ching-Hung Shen, James Lu, James Evans and Alec Robertson. Also worthy of mention are Adam Drake whose influenza virus stock was used for all the infections, and Maria Fragoso who maintained breeding of the 2C GFP RAG1-/- despite many difficulties. I am eternally grateful to Alicia Caron of the MIT CCR histology facility who sectioned all the tissue shown here as well as prepared the H&E slides. Thanks to Roderick Bronson, the CCR veterinary pathologist who helped me understand the histopathology. After several attempts, only advice about immunofluorescence staining from Denise Crowley of the MIT CCR histology facility and from Nicki Watson of the Whitehead Institute Keck Microscopy facility produced results. Thank you. Finally, I would like to thank my family and friends who have encouraged me despite all odds to continue with this research. I am indebted to your love and prayers. This research was funded by the National Science Foundation Graduate Research Fellowship and by the Singapore-MIT Alliance grant.